JOURNAL OF MATERIALS SCIENCE 32 (1997) 375–387

Influence of short-fibre reinforcement on the mechanical and fracture behaviour of polycarbonate/Acylonitrile Butadiene Styrene polymer blend

K. J. DIN, S. HASHEMI
University of North London, School of Polymer Technology, Holloway Road, London N7 8DB, UK

The present study investigated the dependence of various mechanical and fracture properties on the volume fraction, ϕ_f, of the reinforcing glass fibres in Polycarbonate/Acylonitrile Butadiene Styrene (ABS) blends. The addition of glass fibres enhanced the ultimate tensile strength and modulus and reduced elongation (both to yield and to break) and total work of fracture. The elastic modulus was not significantly affected by the loading mode although the ultimate strength was significantly affected, giving flexural strength values of 1.5–1.6 times greater than tensile strengths. The elastic modulus and strength were linear functions of ϕ_f and thus followed the principle of rule of mixtures. The presence of weldlines in specimens had an adverse effect on most tensile properties except for the elastic modulus. Linear elastic fracture mechanics could not be used to assess the resistance to crack propagation of the present range of materials because their behaviour violated the principle assumptions upon which the theory is based. An alternative method was employed where the total work of fracture and the work of fracture corresponding to the maximum load were plotted as a function of initial crack length. These plots were reasonably linear for the polymer and its composites giving values of the resistance to steady state crack propagation J_T and the J integral of maximum load J_m respectively. Values of J_T and J_m decreased with increasing ϕ_f.

1. Introduction

The original purpose of adding mineral fillers to polymers was primarily one of cost reduction. However, nowadays fillers increasingly play a functional role, such as improving the stiffness or surface finish of a polymer product. In particular, the reinforcement of thermoplastic compounds by short fibres has received special attention because of their use in a variety of engineering applications in both the chemical and automotive industries. These materials can be moulded into complex shapes, and when fibre orientation is controlled, the composites achieve good mechanical properties. In general, the stiffness and strength of the polymer matrix are enhanced by the addition of short fibres. It has been shown [1–4] that the dependence of most mechanical properties with the volume fraction of fibres can be described using some modified form of the rule of mixtures which takes into account effects arising from both orientation of the fibres and distribution of fibre lengths through the injection moulded component.

Regarding the fracture of short fibre composites, previous studies [4–9] have indicated that, provided the nature of failure is brittle one may use the linear elastic fracture mechanics parameter, K_c, to determine fracture toughness of these composites. However, when failure is by ductile tearing, as in most toughened matrices, the J-integral approach has been used quite successfully to determine both the fracture toughness, J_c, and also the resistance of the composite to crack propagation. A method which has received little attention, certainly as far as short fibre composite materials are concerned, is the Locus method [10–12]. A recent study by Nabi and Hashemi [13] on glass-bead-filled systems has shown that this method, which in effect is an extension of the J-integral approach, can also be used to determine the resistance of the material to crack propagation. This paper reports and discusses the affect of short glass fibres on a few selected mechanical properties in addition to the fracture behaviour of PC/Acylonitrile Butadiene Styrene blends. In addition, the influence of weldlines on mechanical properties was also investigated.

2. Experimental details

2.1. Materials

The polymer matrix used in this study is a thermoplastic blend of Polycarbonate (PC) and Acylonitrile

0022–2461

Butadiene Styrene (ABS) supplied by Bayer under the trade name Bayblend T45 MN.

2.2. Compounding

The blend was mixed with varying amounts of short glass fibres to produce composites with nominal glass fibre contents of 5%, 10%, 20% and 30% by weight. Compounding was performed in a Brabender twin screw extruder fitted with a die of diameter 4 mm. The melt temperature was 260 °C and the screw speed was 4–7 rpm. The extrudates were then pelletized and dried at 90 °C for 3–4 h before injection moulding.

2.3. Mouldings

Two types of specimens were injection moulded (See Fig. 1);

(1) TENSILE BARS: Dumbell shaped specimens of dimensions $1.7 \times 12.5 \times 125$ mm were produced on a Negri Bossi NB60 with a melt temperature of 260 °C, mould temperature of 78 °C (Table I summarises the moudling conditions). The mould used contained two cavities, a single feed and a double feed cavity in which the two opposing melt fronts meet to form a weldline mid-way along the gauge length.

(2) FLEXURAL BARS: Flexural specimens of dimensions $4 \times 10 \times 120$ mm were moulded using a Klockner Ferromatik F60 injection moulding machine. The processing temperature was 260 °C and the mould temperature was 90 °C (Table I summarises the moulding conditions).

2.4. Fibre length distribution

The fibre length distribution and the exact volume fraction of glass fibres in moulded specimens were determined using the ash test. Small samples were cut from the centre of moulded test specimens and burned in a muffle furnace at 500 °C for 2 h. The remaining fibres were then weighed to determine the weight and volume fraction of fibres. The fibres, were viewed under an optical microscope so that the fibre length could be determined. A series of photographs were taken from which 300–400 fibre lengths were counted. A frequency distribution of the fibre lengths were plotted for each composite (see examples shown in Fig. 2(a and b)) from which the average fibre length, L_f, was determined for each composite.

The exact weight fraction of the fibres, w_f in each composite was also measured using the remaining fibres. The corresponding volume fractions, ϕ_f, were then determined from the following equation;

$$\phi_f = \left[1 + \frac{\rho_f}{\rho_m}\left(\frac{1}{w_f} - 1\right)\right]^{-1} \quad (1)$$

taking the density of matrix, ρ_m, as $1.1\,\mathrm{kg\,m^{-3}}$ and that of the fibre, ρ_f, as $2.5\,\mathrm{kg\,m^{-3}}$.

Fig. 3 shows a plot of the mean fibre length versus volume fraction of the glass fibres. As can be seen, there is a sharp drop in the mean fibre length as the volume fraction of glass fibres exceeds 4.3%. This is probably due to enhanced fibre breakage during the mould filling process, particularly in specimens with higher fibre content.

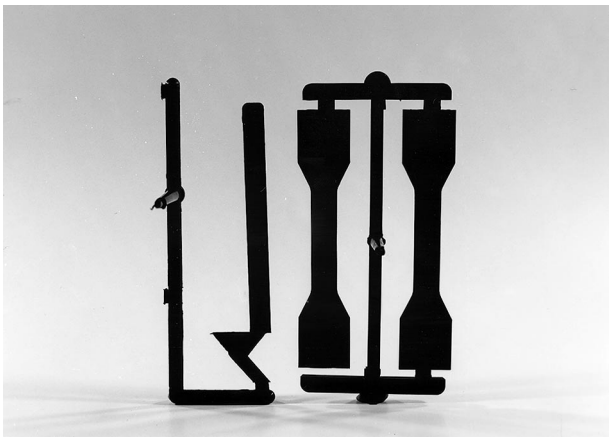

Figure 1 Injection moulded specimens.

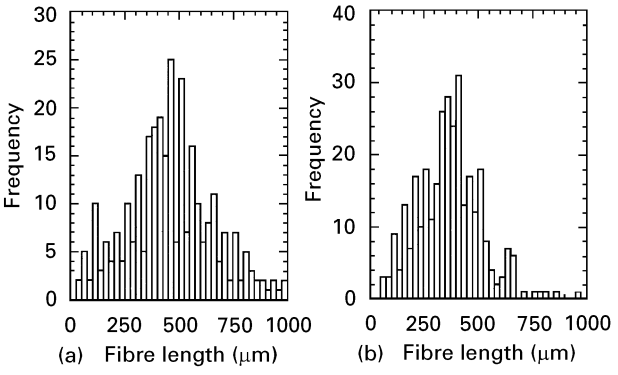

Figure 2 Fibre length distributions at (a) $\phi_f = 4.3\%$ and (b) $\phi_f = 15.3\%$.

TABLE I Processing conditions

Processing Parameters	Dumbell specimens	Flexural Bars
Melt temperature (°C)	250/255/260/265	260/265/270/270
Mould temperature (°C)	78	90
Cooling time (s)	25	25
Holding time (s)	3–5	9
Cycle time (s)	38–40	38–41
Holding pressure ($\times 10^5$ Pa)	15–20	30 ± 2
Injection pressure ($\times 10^5$ Pa)	35–90	30 ± 2

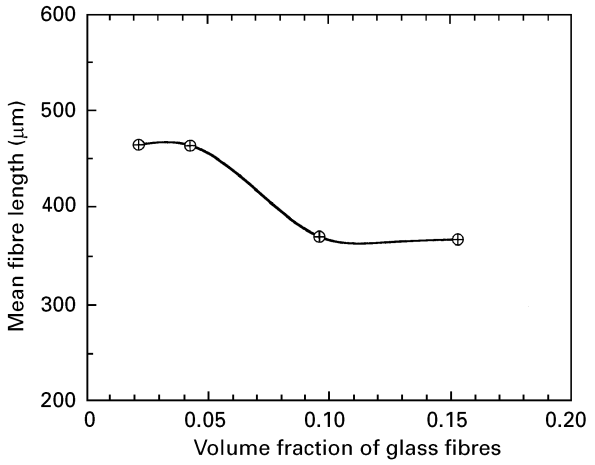

Figure 3 Mean fibre length versus volume fraction of the fibres.

2.5. Testing procedures

2.5.1. Tensile tests

Dumb-bell specimens both with and without weldlines were tested in tension at a crosshead speed of 5 mm per min in an Instron testing machine. The quantities measured from the recorded load–displacement diagrams for the polymer specimens and its composites were; (i) the nominal yield stress calculated on the basis of the maximum load, (ii) the tensile modulus calculated from the initial slope, (iii) the elongation at yield and at break, and (iv) the work of fracture (calculated from the total area under the load–displacement diagram).

2.5.2. Flexure tests

Ultimate strength and modulus in bending mode were measured in three point-bend flexure using rectangular bars with nominal thickness, B, of 10 mm, depth, D, of 4 mm and a loading span, S, of 64 mm as is shown in Fig. 4a. Tests were performed at a constant crosshead speed of 5 mm per min with a load–displacement trace for each specimen being recorded. The flexural strength and modulus were measured from the traces on the basis of the maximum load and initial slope respectively, using linear elastic beam equations.

2.5.3. Impact tests

The impact strengths of both notched and unnotched specimens were measured using rectangular bars with thickness, B, of 4 mm, depth, D, of 10 mm and a loading span of 40 mm (see Fig. 4b). The tests were conducted on a conventional non-instrumented Charpy-type pendulum machine at an impact speed of 3 m s^{-1}. All the notched impact test specimens, contained a V-shaped edge notch having a tip radius of 0.25 mm and a/D of 0.3, where a is the crack.

2.5.4. Fracture toughness

Fracture tests for measuring the material resistance to crack propagation were carried out on single-edge notched bend (SENB) specimens (as in Fig. 4b) under

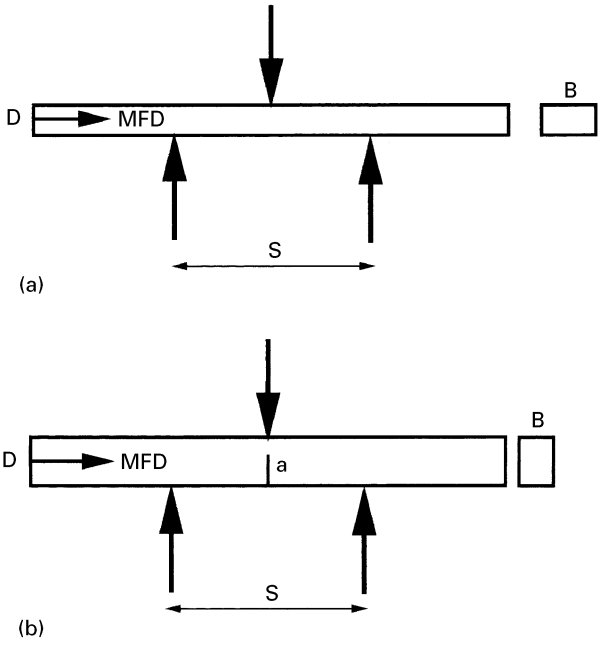

Figure 4 The three-point bend specimen configurations for (a) the flexure test specimen and (b) the SENB specimen

three-point bending at a crosshead speed of 5 mm per min. Specimens were razor notched to various a/D ratios ranging from 0.1–0.7. A load–displacement trace for each specimen was recorded for subsequent analysis.

3. Mechanical properties

3.1. Deformation

Figs 5(a and b) show typical examples of load–displacement diagrams obtained for both the tensile and flexural specimens. As expected, the introduction of glass fibres into the PC/Acylonitrile Butadiene Styrene polymer lowers elongation to yield, e_y, and to break, e_b. This is probably owing to the fact that the specimens are part glass (rigid) and part polymer and all the deformation is predominantly from the polymer. These changes are usually associated with the increasing brittleness of the composite which is clearly demonstrated by the load–displacement diagrams. The broken tensile test specimens shown in Fig. 6, further indicate that while the unfilled material forms a neck, the filled materials having a volume fraction of glass greater than 2.2 vol% fracture in a brittle manner.

Table II summarizes the deformation behaviour of the unfilled and filled polymer. These values are plotted in Fig. 7 as a function of ϕ_f, evidently, filled materials having volume fraction of glass greater than 2.2 vol% break at a strain value which is lower than the yield strain of the unfilled polymer. Increasing the filler concentration reduced the yield and the breaking strains attainable in the composite.

In bending mode, a completely brittle failure was obtained when the volume fraction of glass fibres exceeded 4.3% as is shown in Fig. 5b. Matrix and composite specimens with $\phi_f = 2.2\%$, did not break under the testing conditions used here. Values of maximum strain at yield and at break are given in Table II

TABLE II Summary of the deformation properties

ϕ_f (%)	0	2.2	4.3	9.6	15.3
Tensile yield strain (%)	5.10 (0.10)	4.18 (0.06)	brittle	brittle	brittle
Tensile breaking strain (%)	88.29 (4.43)	5.51 (0.42)	3.21 (0.18)	2.89 (0.14)	2.77 (0.21)
Flexural yield strain (%)	5.46 (0.07)	4.91 (0.07)	3.69 (0.03)	brittle	brittle
Flexural breaking strain (%)	no break	no break	4.50 (0.13)	2.68 (0.06)	2.16 (0.06)

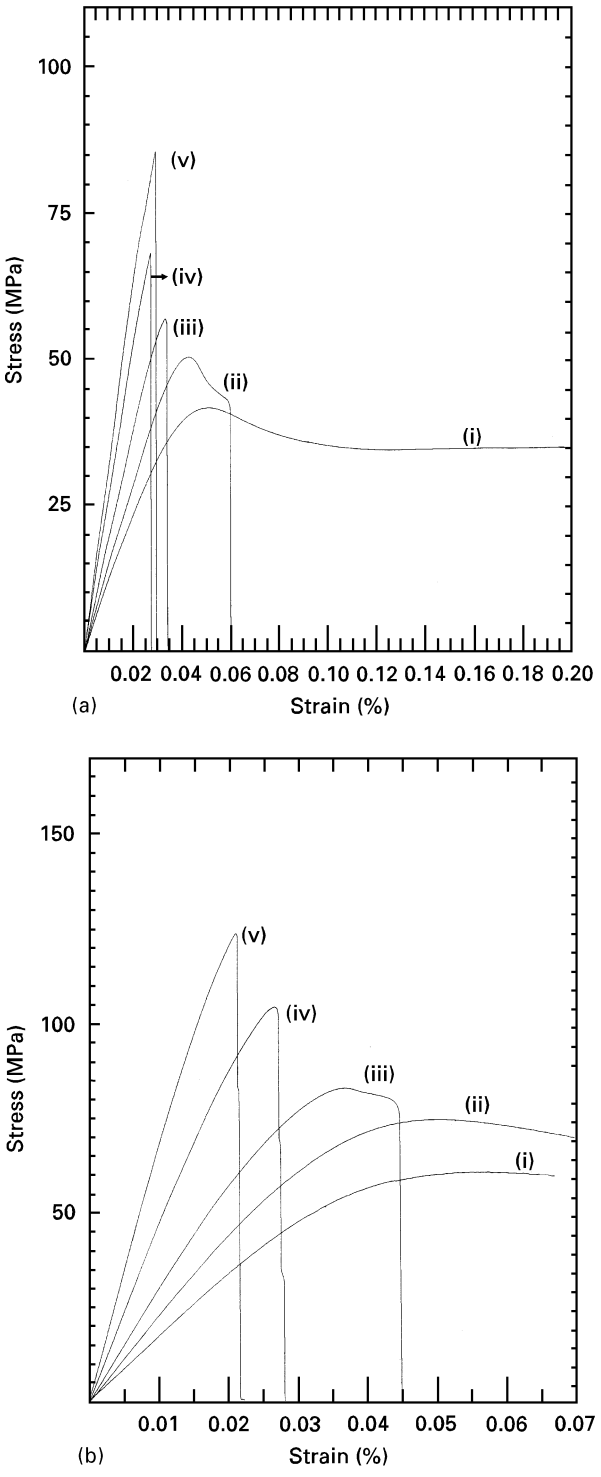

Figure 5 Typical load–displacement diagrams; (a) tensile (b) flexural data were taken for (i) resin and for ϕ_f values of (ii) 2.2% (iii) 4.3% (iv) 9.6% and (v) 15.3%

and are plotted as a function of ϕ_f in Fig. 7, where it can be seen that they decrease with increasing ϕ_f. As in tension mode, the breaking strain of the composites is lower than the yield strain of the polymer matrix;

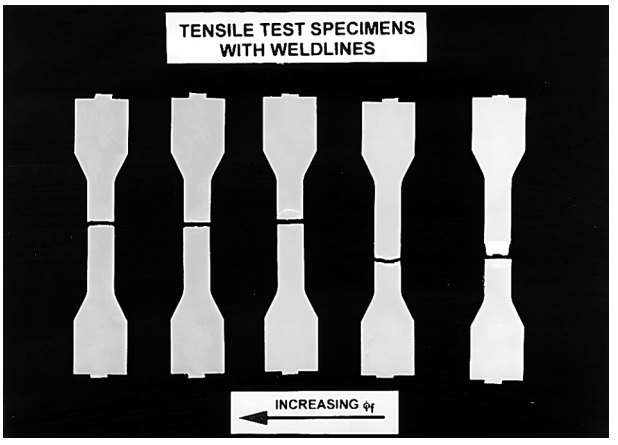

Figure 6 Tensile test pieces.

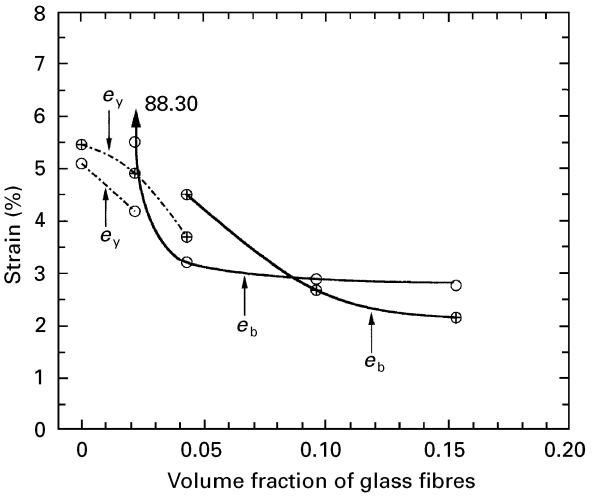

Figure 7 (○) Tensile and (⊕) flexural strains versus the volume fraction of glass fibres.

indicating that the deformation of the polymer matrix is severely reduced in the presence of fibres.

3.2. Work of fracture

The work of fracture or strain energy, U, given by the area enclosed by the tensile load–displacement diagram and the x-axis, are plotted in Fig. 8 as a function of ϕ_f. Clearly, the addition of only 2.2 vol% glass fibres to the polymer matrix reduces work of fracture from 52 to 2.93 J. However, as shown in Fig. 8 (inserted plot), the work of the fracture starts to rise as ϕ_f exceeds 4.3%. This is because after this volume fraction, any reduction in the breaking strain is more than compensated for by the increase in tensile strength (see section 3.4).

3.3. Elastic properties

Table III summarizes the initial elastic modulus of the polymer and its composites in tension and in bending modes.

Results indicate that the modulus of the unfilled polymer is enhanced by the addition of glass fibres. There is however, a considerable difference between the values measured in tension and those measured in flexure with flexural values being consistently higher than tensile values. It is noteworthy, that tensile and flexural specimens were made using not only two different injection moulding machines but also two different types of mould geometry. Thus on the basis of the understanding that fibre orientation within the two mouldings may differ, one may expect some differences between the two measured values. However, in the opinion of the authors, the difference between the tensile and the flexural moduli is mainly due to the way in which tensile values were measured. The measurements here were based upon clamp separation, and as such could give erroneous results, owing to slippage of the test specimen in the clamps. We were concerned when tensile modulus values were significantly affected as the sample gauge length was varied. This was apparently due to machine compliance and other factors which had their origin in other remote parts of the machine, such as the clamps and gear train. These effects were considered in their totality by the following relationship, which is based on the assumption that the strains in the specimen and the instrument are additive:

$$\frac{1}{E_{app}} = \frac{1}{E_{act}} + \frac{kA}{L} \tag{2}$$

where E_{app} is the apparent elastic modulus, E_{act} is the actual elastic modulus, k is the instrument constant, and A and L are the cross-sectional area and the gauge length of the specimen. According to this equation, $1/E_{app}$ is a linear function of A/L from which E_{act} can be ascertained from the inverse of the intercept at $A/L = 0$, and k from the slope of the line. Therefore, a series of tensile tests were performed in which the specimen gauge length varied between 10–90 mm. The results obtained from these tests are plotted in Fig. 9 as $1/E_{app}$ versus A/L. Clearly the plots are essentially linear from which E_{act} can be ascertained with a reasonable degree of accuracy (see Table III). The comparison between E_{act} and the flexural modulus as illustrated in Fig. 10 indicates, that a loading mode does not affect elastic properties of the polymer or its composites.

It is also evident from Fig. 10, that the variation of the elastic modulus (tensile or flexural) with respect to ϕ_f is reasonably linear suggesting that the behaviour follows some form of the rule of mixtures. Using the simplest approach, the modulus of a short glass fibre reinforced composite, E_c, as a function of ϕ_f, may be obtained from the following rule of mixtures [2];

$$E_c = \eta_o \eta_L \phi_f E_f + (1 - \phi_f)\, E_m \tag{3}$$

where, E_f, is the modulus of the reinforcing fibres and E_m, is the modulus of the surrounding matrix. The factor, η_o, considers the orientation efficiency of the reinforcing fibres (having a value of 1 for aligned-longitudinal, 0 for aligned-transverse) and the factor, η_L, considers the reinforcing effectiveness of the short

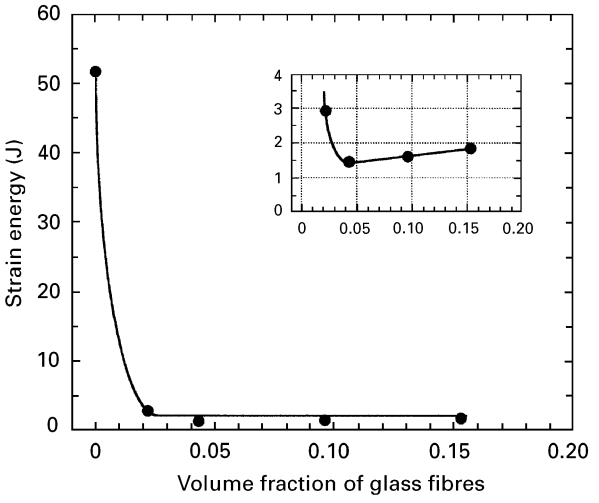

Figure 8 Strain energy versus the volume fraction of glass fibres.

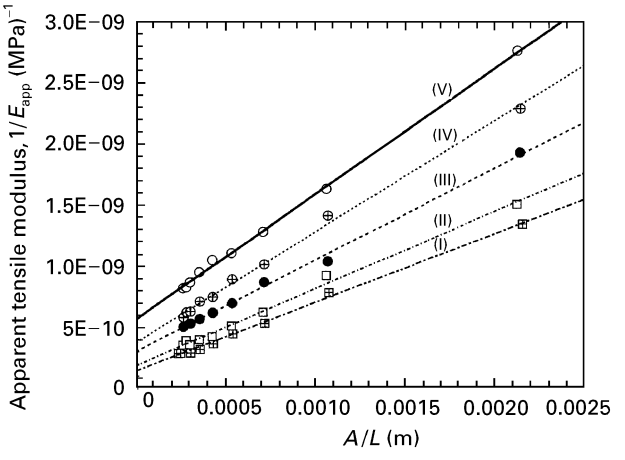

Figure 9 Apparent tensile modulus versus A/L for the polymer and its composites. Data are presented for ϕ_f values of (i) 0.153 (ii) 0.096, (iii) 0.043, (iv) 0.022 and (v) 0.

TABLE III Summary of the elastic properties

ϕ_f (%)	0	2.2	4.3	9.6	15.3
Flexural modulus (GPa)	1.77 (0.02)	2.33 (0.02)	3.06 (0.03)	4.82 (0.06)	7.04 (0.08)
Tensile modulus, E_{app} (GPa)	1.16 (0.07)	1.65 (0.05)	1.90 (0.08)	2.52 (0.11)	3.13 (0.18)
Tensile modulus, E_{act} (GPa)	1.78	2.68	3.33	5.40	7.05
k (MPa) $^{-1}$	1.03	0.91	0.75	0.63	0.56

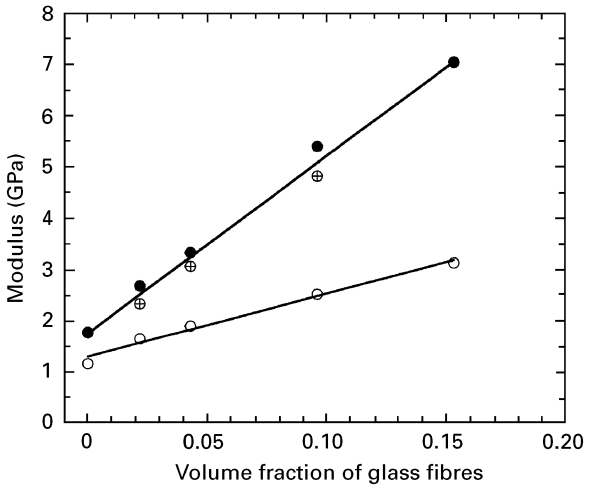

Figure 10 The tensile modului; (○) E_{app} and (●) E_{act} and (⊕) flexural modulus versus the volume fraction of glass fibres.

fibres which can be estimated from [2];

$$\eta_L = 1 - \frac{\tanh x}{x}$$

where

$$x = \frac{L_f}{2}\left(\frac{8\,G_m}{E_f d^2 \ln(2R/d)}\right)^{1/2} \quad (4)$$

where G_m is the shear modulus of the matrix, d, is the diameter of the fibres and $2R$ is centre to center spacing of the fibres which for the assumed hexagonal packing arrangement is related to the diameter and volume fraction of the fibres by the following relationship;

$$\frac{d}{2R} = \left(\frac{2(3)^{1/2}\,\phi_f}{\pi}\right)^{1/2} \quad (5)$$

Assuming that the values of η_L and η_o are relatively constant for a given composite system, then Equation 3 can be rearranged to give;

$$E_c = E_m(1 + \gamma\phi_f)$$

where

$$\gamma = \frac{\eta_o \eta_L E_f}{E_m} - 1 \quad (6)$$

The best straight line fitted to the data in Fig. 10 may be represented by;

$$E_c = E_m(1 + 19.82\phi_f) \quad (7)$$

having a regression coefficient of 0.98. Using the slope of this line and taking the diameter of the fibre, d, as 10 μm, the Poisson's ratio of the matrix, v_m as 0.35, the tensile modulus of the fibre, E_f, as 76 GPa and the shear modulus of the matrix, G_m, as $E_m/2(1 + v_m)$, we obtained η_L value to be 0.78 and η_o to be 0.62 for the composite systems under investigation (see Table IV).

It is noteworthy, that the η_o values show no variation with respect to L_f and further more they agree quite well with values reported by Voss and Fredrich [3] and those more recently reported by Hashemi *et al.* [4] albeit for different composite systems.

TABLE IV Orientation and fibre length efficiency parameters

ϕ_f	0.022	0.043	0.096	0.153
L_f (μm)	467.0	464.0	370.0	367.0
$d/2R$	0.156	0.218	0.325	0.411
x	4.46	4.917	4.567	5.088
η_L	0.78	0.78	0.78	0.80
η_o	0.62	0.62	0.62	0.61

3.3. Ultimate strength

A summary of the ultimate tensile and flexural strengths of the polymer matrix and its composites is given in Table V.

As can be seen, the ultimate strength of the polymer matrix is enhanced by the addition of glass fibres. As is illustrated in Fig. 11, the tensile and flexural strengths both vary linearly with ϕ_f. Apparently, the flexural strength of the polymer and its composites is always greater than the corresponding tensile strengths. The ratio of the two strengths (flexural/tensile) which is often referred to as the "modulus of rupture, M. O. R" varied between 1.51–1.60 for the present range of ϕ_f values (see Table V). According to observations based on analysis of plastic bending (or plastic collapse), rectangular cross-section beams can carry an additional 50% moment to that which is required to produce initial yielding at the edges of the beam section before a fully plastic hinge is formed. This suggests that the flexural strength under the plastic collapse condition is expected to be 1.5 times that of the tensile yield strength. Indeed the flexural load–displacement diagrams of the polymer matrix and the composite with glass contents of 2.2 vol% indicate that the difference between the two strengths is due to the occurrence of plastic yielding during the flexure test where deformation for both materials was completely ductile through out the test (see Fig. 7b). As for composites with glass fibre contents greater than 2.2 vol%, where in fact failure under both loading modes was brittle, the difference between the flexural and tensile values can be attributed to factors such as;

(i) A nonuniform stress distribution in bending as opposed to a uniform stress distribution in tension; This implies that in a tensile test the whole volume of the specimen is subjected to the tensile state and thus the measured stress value is the mean value of stress across the specimen thickness. Whereas in bending, the maximum stress is reached only on the extreme tensile face of the specimen.

(ii) statistical aspect of fracture; It has been observed by Weibull [14] that the strength of a brittle material is strongly dependent upon volume and stress distribution and because of this, the average maximum stress at failure in bending is expected to be higher than that of an identical specimen in tension since the number of flaws in the outer surface of the specimen is usually lower and their sizes smaller than in the bulk of the specimen.

The linearity of the tensile and flexural strengths with ϕ_f indicate that these quantities, as with the elastic modulus, should also obey some form of the rule of mixtures. According to Kelly and Tyson [1]

TABLE V Summary of the tensile and flexural strengths

ϕ_f (%)	0	2.2	4.3	9.6	15.3
Tensile strength (MPa)	40.4 (0.23)	50.61 (0.28)	52.36 (3.48)	66.36 (3.1)	78.39 (3.2)
Flexural strength (MPa)	61.97 (0.56)	76.48 (0.50)	83.68 (1.11)	105.6 (1.5)	124.43 (2.5)
M.O.R	1.53	1.51	1.60	1.59	1.59
η_L		0.63	0.63	0.70	0.70
η_o (tensile test)		0.28	0.28	0.35	0.35
η_o (flexure test)		0.49	0.49	0.60	0.60

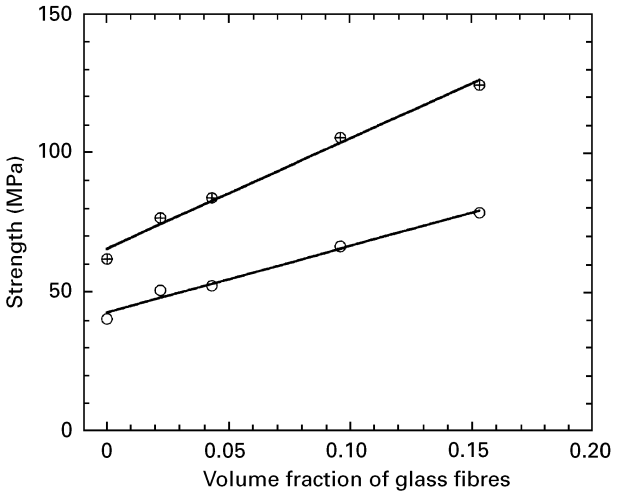

Figure 11 (○) Tensile and ⊕ flexural strengths versus the volume fraction of glass fibres.

ultimate strength of the short fibre composites, σ_c, may be related to ϕ_f according to the following rule of mixtures;

$$\sigma_c = \eta_L \eta_o \phi_f \sigma_f + \sigma_m(1 - \phi_f) \quad (8)$$

where σ_f is the ultimate strength of the fibres and σ_m is ultimate strength of the surrounding matrix. The first term in Equation 8 describes the load-carrying capacity of the fibres and the second term the strength of the surrounding matrix. The factor η_o represents the orientation efficiency of the short fibres and the factor η_L represents the reinforcing effectiveness of the short fibres. For the case in which the average fibre length, L_f is less than the critical value, L_c, η_L is given by [1–2];

$$\eta_L = \frac{L_f}{2L_c} \quad (9)$$

and for $L_f > L_c$ it is given by [1, 2]

$$\eta_L = 1 - \frac{L_f}{2L_c} \quad (10)$$

where, L_c, can be calculated from the following equation;

$$L_c = \frac{d\sigma_f}{2\tau_m} \quad (11)$$

Taking the tensile strength of the fibres, σ_f, as 2.47 GPa and the shear strength of the matrix, τ_m, as half its tensile yield strength (i.e., 20 MPa), the critical fibre length for the composite system used here was estimated as 620 μm, which is higher than the average fibre length values shown in Fig. 3. Accordingly, we may write;

$$\sigma_c = \sigma_m\left[1 + \left(\frac{L_f \sigma_f \eta_o}{2L_c \sigma_m} - 1\right)\phi_f\right] \quad (12)$$

Thus, provided that the term inside the bracket remains reasonably constant for a given composite system, a linear relationship between σ_c and ϕ_f is expected as was observed in our measurements. According to Fig. 11, the variation of tensile strength with ϕ_f can be reasonably approximated by;

$$\sigma_c = \sigma_m(1 + 5.44\phi_f) \quad (13)$$

and that of the flexural strength by;

$$\sigma_c = \sigma_m(1 + 6.19\phi_f) \quad (14)$$

where in Equation 13, σ_m represents the tensile strength of the surrounding polymer matrix and in Equation 14 it represents the flexural strength of the surrounding matrix.

On the substitution of the slopes of these lines into Equation 12, we obtain the η_o values that are listed in Table V. In contrast to the analysis based on elastic modulus, where η_o values were found to be independent of ϕ_f and the loading mode, the analysis based on strength values suggests that η_o is not only strongly dependent on ϕ_f but is affected by the mode of loading. The variation of η_o with ϕ_f stems from the observed variation of L_f with ϕ_f as illustrated in Fig. 3. The influence of the loading mode which is highlighted by the higher η_o values obtained in flexure rather than in tension is caused by the fact that the calculated critical fibre length was based upon the tensile yield stress of the matrix rather than its flexural value. This causes some inconsistency when flexural values are used to evaluate η_o on the basis that they are 1.5–1.6 times higher than tensile strengths.

3.4. Impact

Fig. 12 shows the variation of notched and unnotched impact strengths of the polymer and its composites as a function of ϕ_f. Since the unnotched specimens of the polymer matrix, did not break under the testing conditions used, it was not possible to measure its impact strength value. There is nevertheless, a clear indication, that the impact strength of the polymer matrix decreases drastically with increasing ϕ_f. The results also suggest, that while the notched impact strength of the polymer matrix decreases continuously with

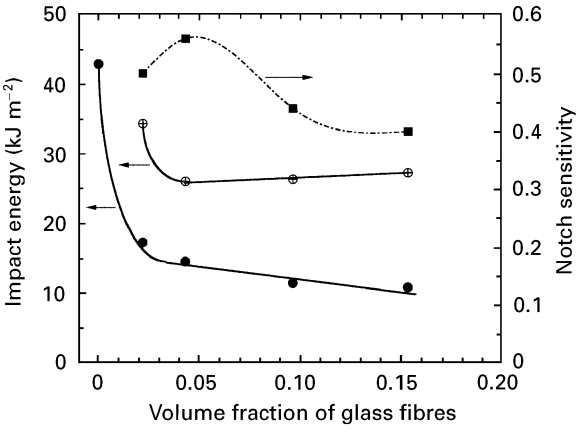

Figure 12 Impact energy and notch sensitivity versus the volume fraction of glass fibres. Data are presented for (●) notched and (⊕) unnotched specimens.

increasing ϕ_f, the unnotched impact strength shows a minimum value at around a ϕ_f value of about 5–6%. Over this range, the ratio of two impact strengths (notched/unnotched) known as the notch sensitivity parameter, is maximum at a value of 0.55 (see Fig. 12) and thus composites within this range are expected to be less vulnerable to notches than the polymer matrix or composites with volume fractions of glass fibres out side the range.

It is noteworthy, that although the polymer matrix is extremely notch sensitive, its notched impact strength value is still superior to that of its unnotched composites.

4. Effect of weldlines on mechanical properties

Typical examples of load–displacement diagrams and the broken test bars for tensile specimens containing a weldline are depicted in Figs. 13 and 14 respectively. As can be seen the behaviour of the specimens with weldlines can be characterized as being brittle with failure occurring at the weldline. This indicates that the weldlines in these specimens generate a source of mechanical weakness.

Table VI, summarises the quantities measured from tensile load–displacement diagrams of the welded specimens. To compare the weld and weld free results, a parameter called the "weldline integrity, F" was defined as;

$$F = \frac{\text{measured quantity with a weldline}}{\text{measured quantity without a weldline}} \quad (15)$$

Using this parameter, a ratio of unity represents weldline insensitivity and lower values represent degrees of vulnerability. Since the welding integrity values given in Table VI, are all less than unity, all quantities listed are affected to some extent by the presence of weldlines in the specimen. In fact, the only quantity which remained unaffected by the weldline was the tensile modulus with F values ranging from 0.98–1.0.

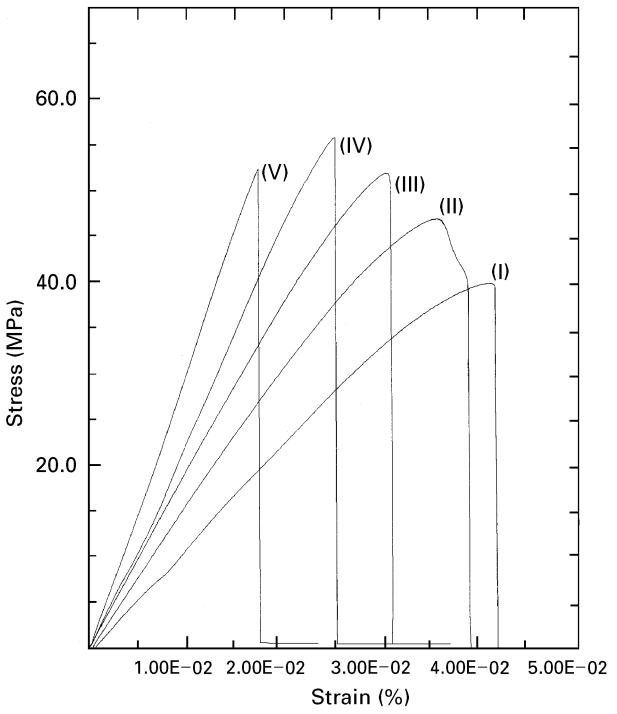

Figure 13 Tensile load–displacement diagrams for specimens with a weldline. Data are presented for (i) the resin and for ϕ_f values of; (ii) 2.2%, (iii) 4.3%, (iv) 9.6% and (v) 15.3%

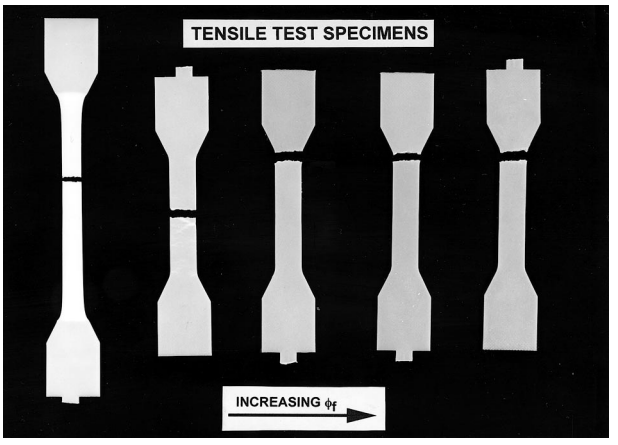

Figure 14 Tensile test specimens with a weldline.

It is worth noting that although the weldline had no significant effect on the tensile strength of the polymer matrix, it became significant in the case of the breaking strain and the work of fracture, where the weldline integrity parameter for both measured quantities was found to be as low as 0.05. However, as shown in Figs. 15 and 16, the weldline integrity parameter for both quantities rises initially with a small addition of glass fibres, with an optimum value being reached at around a ϕ_f value of 4.3%. Moreover, as is shown in Fig. 17, the tensile strength of the welded specimens initially increases with increasing ϕ_f but then remains almost independent of ϕ_f at a stress value of 51 MPa. On the basis of these results, the observed reduction in the work of fracture (strain energy) with increasing ϕ_f is attributed mainly to the reduction in tensile strain across the weldline caused by fibres aligning

TABLE VI Summary of the tensile properties of welded specimens

ϕ_f (%)	0	2.2	4.3	9.6	15.3
Tensile yield strain (%)	4.22 (0.26)	3.63 (0.05)	brittle	brittle	brittle
Tensile breaking strain (%)	4.41 (0.56)	3.96 (0.06)	3.01 (0.10)	2.25 (0.06)	1.66 (0.15)
F	0.05	0.72	0.96	0.78	0.60
Energy (J)	1.64 (0.22)	1.75 (0.05)	1.27 (0.08)	0.99 (0.08)	0.75 (0.14)
F	0.03	0.60	0.87	0.62	0.41
Tensile Strength (MPa)	39.97 (1.18)	47.05 (0.35)	48.21 (1.68)	51.93 (2.87)	51.0 (3.56)
F	0.94	0.93	0.92	0.78	0.65

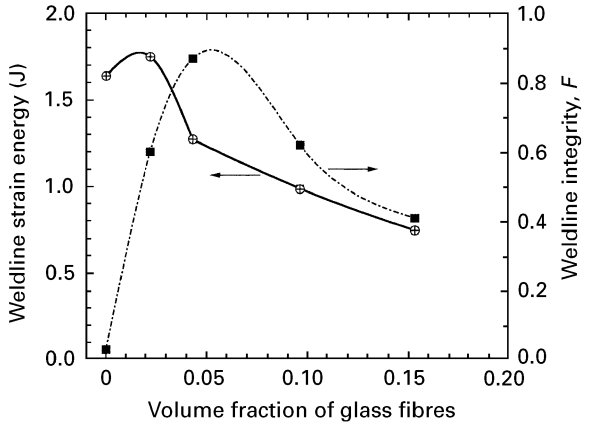

Figure 15 Weldline strain energy and weldline integrity parameter versus the volume fraction of glass fibres.

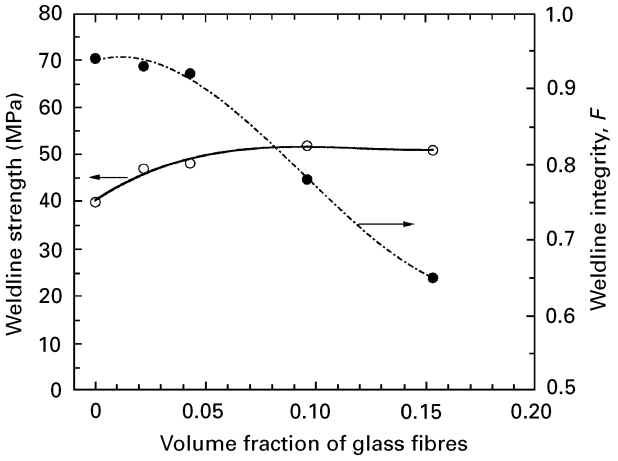

Figure 17 Weldline strength and integrity parameter versus the volume fraction of glass fibres.

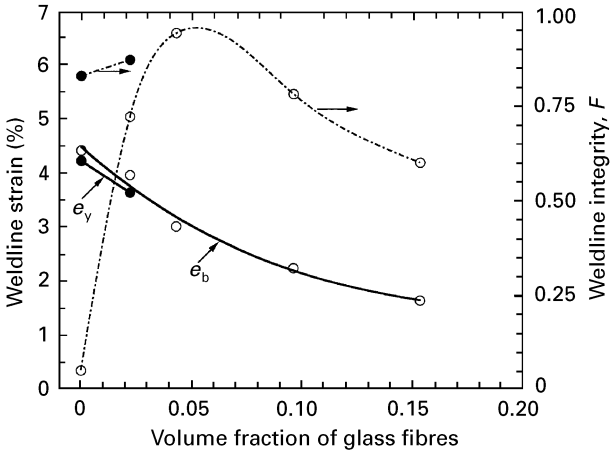

Figure 16 Weldline strain and integrity parameter versus the volume fraction of glass fibres.

preferentially parallel to the weldline and thus normal to the direction of the applied stress. It should be noted that the tensile strength of the welded composites is still greater than that of the matrix without the weldline. This indicates that as far as tensile strength and modulus measurements are concerned, the addition of glass fibres is still beneficial even in the presence of a weldline.

5. Fracture toughness

Fig. 18(a–d) show typical SENB load–displacement diagrams of the polymer matrix and its composites with varying cracks. The plots show that whereas crack growth is essentially unstable for short crack lengths (composites only), it is stable for long crack lengths.

To determine the fracture toughness, K_c, we used the well known linear elastic fracture mechanics equation [15];

$$K_c = \sigma_c Y a^{1/2} \quad (16)$$

where σ_c is the gross applied stress at fracture, a is the initial crack length and Y is a geometrical correction factor introduced to account for finite width effect [15]. Fig. 19 shows the variation of K_c calculated at maximum load with a/D for the polymer and its composites. Evidently, these values are dependent on the length of the initial crack. Therefore K_c in its simplest form as given by Equation 16 was considered inappropriate for characterizing the fracture resistance of these materials.

Consequently, we used alternative methods for characterizing the fracture resistance. Two methods were considered; the *J*-integral and the locus method. The former was used only to study the fracture behaviour of the polymer, whereas the latter was used to study that of the polymer and its composites.

5.1. *J*-integral

The multiple specimen *R*-curve (resistance curve) technique (ASTM E813-87 [16]), was used to determine the critical value of the *J*-integral, J_c, for crack initiation and the resistance to crack propagation of the

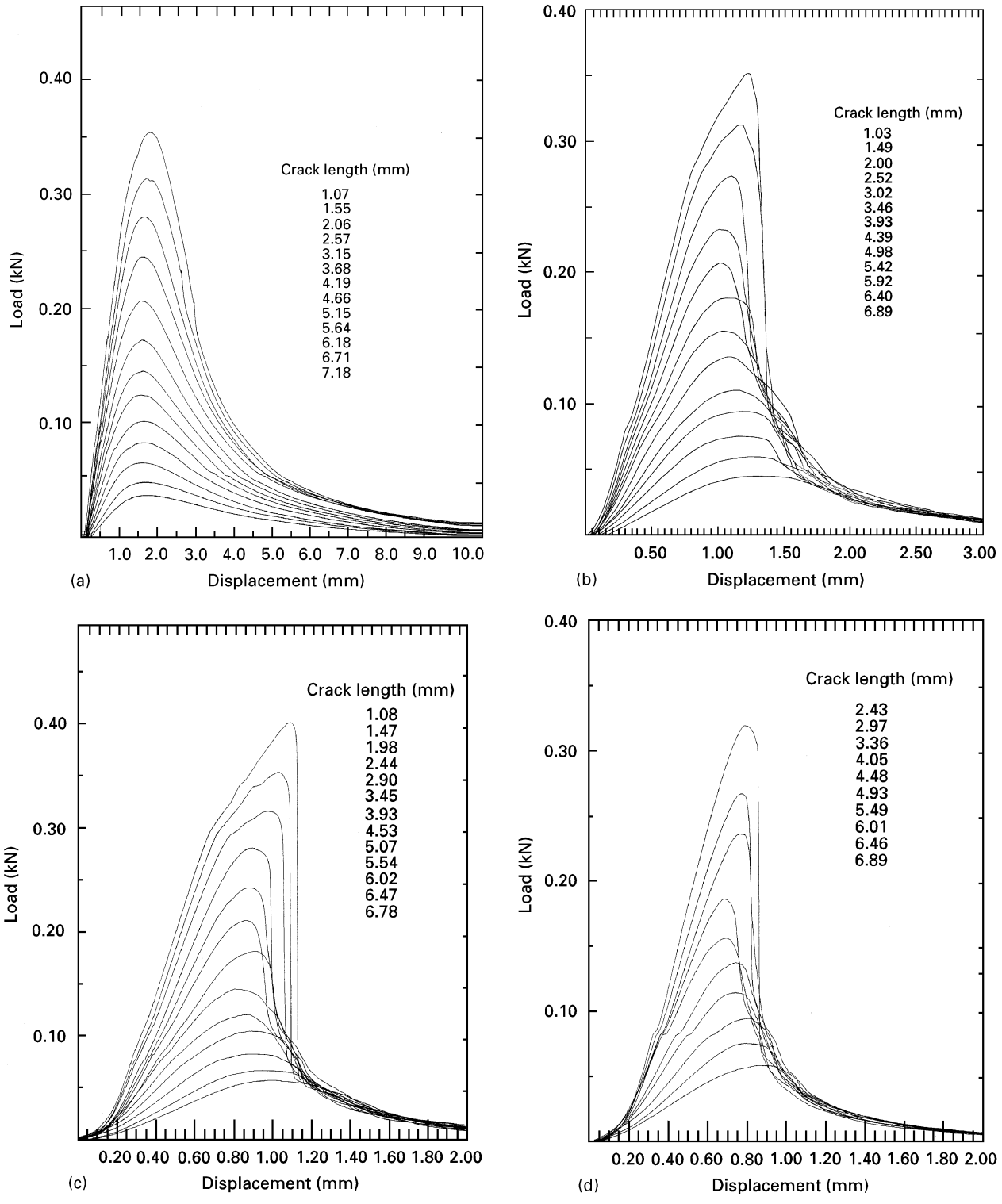

Figure 18 Typical SENB load–displacement diagrams for various crack lengths; (a) PC/ABS polymer (b) $\phi_f = 0.043$ (c) $\phi_f = 0.096$ (d) $\phi_f = 0.153$

polymer matrix. For this purpose several SENB specimens with a/D of 0.5 were tested over a loading span of 40 mm (i.e. a span-to-depth ratio of 4 : 1) at a crosshead speed of 5 mm per min. The specimens were loaded to various displacements corresponding to different crack growth lengths, Δa, and then unloaded. After fully unloading, each specimen was frozen in liquid nitrogen and broken under impact. The crack growth length of the broken specimen was measured by using a travelling microscope.

According to Rice [17]and Begley and Landes [18], the J-integral can be interpreted as the change in potential energy with crack growth, which can be expressed as;

$$J = -\frac{dU}{Bda} \tag{17}$$

where B is the specimen thickness, a, is the crack length and U is the potential energy which can be obtained by measuring the area under the load–displacement curve.

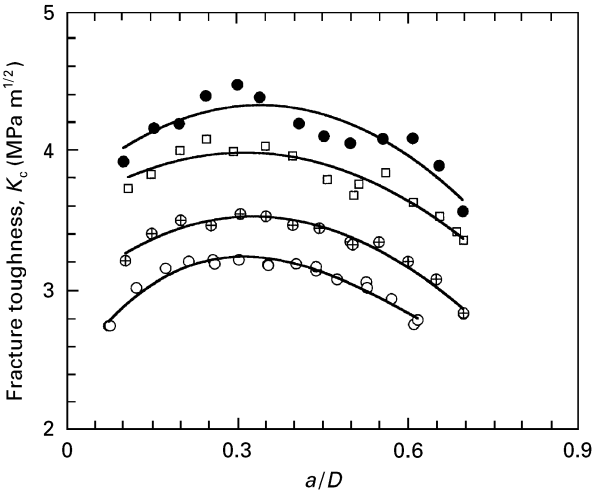

Figure 19 Fracture toughness versus a/D for the polymer and its composites. Data are presented for: (○) PC/ABS, (⊕) $\phi_f = 4.3\%$ (□) $\phi_f = 9.6\%$ and $\phi_f = 15.3\%$.

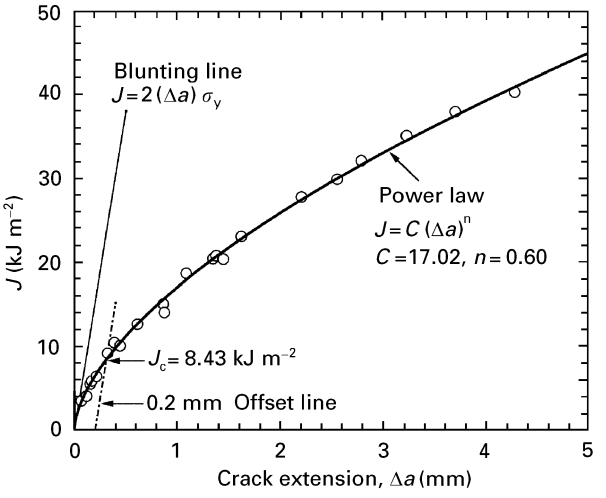

Figure 20 J versus crack extension for the polymer.

The multi-specimen method is based directly on the interpretation of the J-integral as expressed by Equation 17. Sumpter and Turner [19] expanded this equation in the following form;

$$J = J_e + J_p \tag{18}$$

where J_e and J_p are the elastic and plastic components of J respectively. For an a/D ratio of 0.5 and span of $4D$, the above equation can be reduced to the following;

$$J = \frac{2U_e}{B(D-a)} + \frac{2U_p}{B(D-a)} = \frac{2U}{B(D-a)} \tag{19}$$

where U_e and U_p are the elastic and plastic components of the total energy U.

Fig. 20 shows a J versus Δa curve for the polymer. The data is fitted using the power law equation recommended by ASTM E813-87 namely,

$$J = C\Delta a^n \tag{20}$$

with $C = 17.023$ and $n = 0.603$. The critical value of $J(J_c)$ is now located at the intersection of the power law fitted line and the 0.2 mm-blunting-offset line. This gave a value for J_c of 8.43 kJm^{-2} corresponding to a Δa of 0.31 mm. The J value corresponding to the maximum load, J_m was measured as 10.27 kJm^{-2}.

5.2. Locus method

This method also evaluates J_c but utilizes the locus of crack initiation points on load-displacement records or any other relevant energy value from which the locus line can be constructed [10–13]. This method partitions the fracture energy along the locus line based on the same energy rate interpretation as that given by Equation 17. According to this equation, if the value of J along a defined locus line is constant, then the plot of U (or U/B) versus crack length, a, should be linear, where U, is the area enclosed by the locus line, the load–displacement curve and the x-axis (displacement axis).

However, using this method for determining J_c at crack initiation, requires an accurate determination of the onset of crack growth on the load–displacement curve. Such identification often gives erroneous results if carried out visually. Because of this, we constructed the locus-line of the maximum load points as opposed to initiation points. Using these maximum load points J_m, was determined using the following equation;

$$J_m = -\frac{1}{B}\frac{dU_m}{da} \tag{21}$$

where U_m is the area surrounded by the locus line of the maximum load points, the load–displacement curve and the x-axis.

The resistance to steady state crack propagation, J_T may also be obtained from Equation 21 if the total energy, U_T, required to fracture each specimen is known. The U_T for each specimen can be ascertained from the total area enclosed by the load–displacement record and the x-axis. If J_T is constant for steady crack growth, then a plot of U_T versus a should be linear and the slope of this line will yield J_T in accordance with Equation 21.

Fig. 21(a–d) show plots of U_m/B and U_T/B versus the initial crack length, a, for the polymer and its composites respectively. As can be seen the variations are linear, particularly for a/D ratios greater than 0.2, where crack growth is stable. The slopes of these lines gave the J_m and J_T values listed in Table VII. These values are plotted in Fig. 22 as a function of ϕ_f, where it can be seen that they decrease with increasing ϕ_f. It is worth noting that the value of J_m for the polymer as obtained using the J-integral (value given in the bracket) agrees closely with that obtained by use of the locus method.

6. Conclusion

The dependence of various mechanical and fracture properties on the volume fraction, ϕ_f, of the reinforcing glass fibres in polycarbonate/Acylonitrile

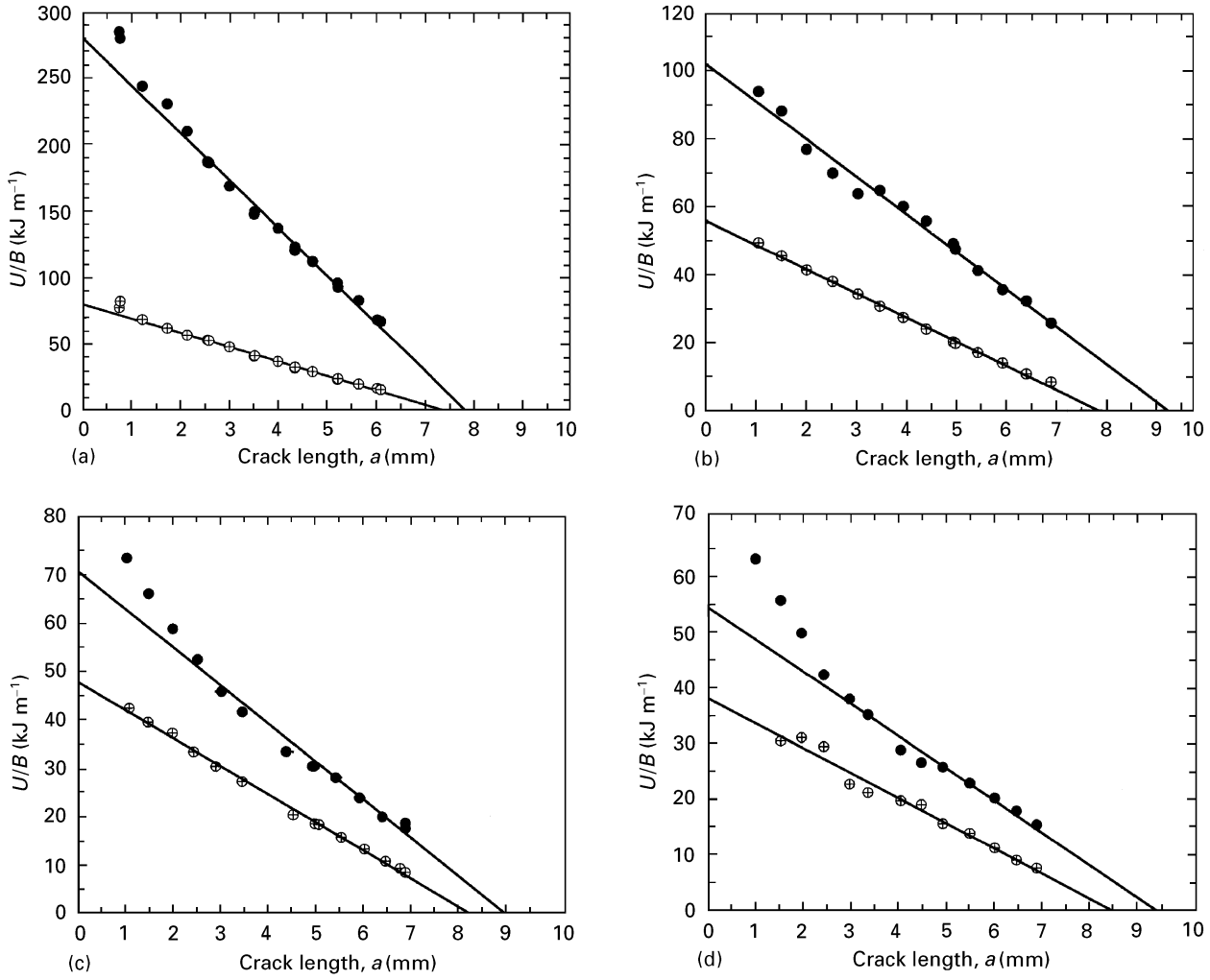

Figure 21 (●) U_T/B and (⊕) U_m/B versus crack length for; (a) PC/ABS polymer (b) $\phi_f = 0.043$ (c) $\phi_f = 0.096$ (d) $\phi_f = 0.153$

TABLE VII J_m and J_T values

ϕ_f (%)	J_m (kJm^{-2})	J_T (kJm^{-2})
0	10.68 (10.27)	35.66
4.3	7.07	11.0
9.6	5.77	7.78
15.3	4.49	5.78

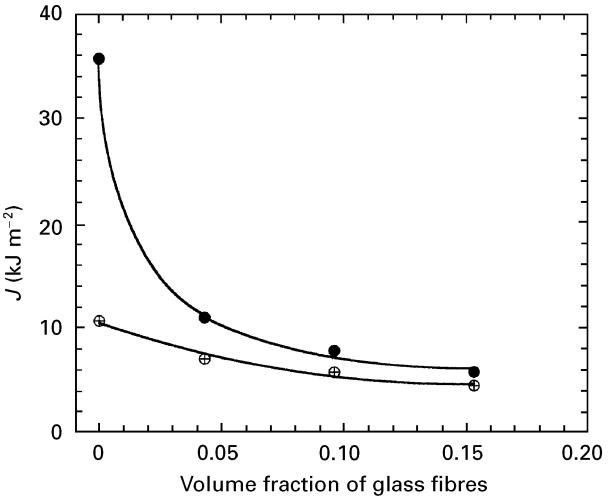

Figure 22 (●) J_T and (⊕) J_m versus the volume fraction of glass fibres.

Butadiene Styrene blend was investigated in tension and in bending. Results indicated that the addition of glass fibres;

(i) enhances ultimate tensile and flexural strengths of the polymer matrix. Variation for both strengths was linear with respect to ϕ_f and thus obeying the rule of mixtures for strengths. It was found also that the strengths were greater in flexure than in tension.

(ii) enhances the elastic modulus of the polymer. The elastic modulus was not affected by the loading mode and was found to be a linear function of ϕ_f which was subsequently described by the rule of mixtures.

(iii) reduces the elongations to yield and to break as well as strain energy (total work of fracture) of the polymer matrix.

(iv) reduces the notched and unnotched impact properties of the polymer matrix.

(v) reduces fracture resistance of the polymer matrix.

The influence of a weldline on the tensile properties was also investigated. The results obtained indicated that apart from the elastic modulus which showed no significant variation with a weldline, other quantities measured were affected by the presence of the weldline

in the specimens. Nevertheless, it was found that the weldline strength of the glass filled polymer was always greater than that of the weldfree polymer. Thus indicating that fibres are beneficial even in the presence of weldlines.

References

1. A. KELLY and W. R. TYSON, *J. Mech. Phys. of Solids.* **6** (1965) 13.
2. D. HULL, "*Introduction to composite materials*", (Cambridge University Press) Cambridge 1981.
3. H. VOSS and K. FRIEDRICH, *J. Mater. Sci.* **21** (1986) 2889.
4. S. HASHEMI, M. T. GILBRIDE and J. HODGKINSON, *ibid* (in press).
5. P. W. R. BEAUMONT and D. C. PHILLIPS, *ibid*. **7** (1972) 682.
6. S. HASHEMI and J. MUGAN, *ibid.* **28** (1993) 3983.
7. A. CHRYSOSTOMOU and S. HASHEMI, *ibid*., **31** (1996) 1183–1197.
8. K. FRIEDRICH, R. WALTER and H. VOSS, *Composites* **17** (1986) 205.
9. K. FRIEDRICH, *Composites Sci and Technol.* **1** (1985) 43.
10. B. H. KIM and C. R. JOE, *Polymer Testing.* **7** (1987) 355.
11. D. M. OTTERSON, B. H. KIM and R. E. LAVENGOOD, *J. Mater. Sci.* **26** (1991) 1478.
12. *Idem*, *ibid*, **26** (1991) 4855.
13. Z. U. NABI and S. HASHEMI, *ibid* (in press).
14. W. WEIBULL, *J. Appl. Mech.* **18** (1951) 293.
15. W. F. BROWN and J. E. SRAWLEY, " *Plan strain crack toughness testing of high strength metallic materials*". ASTM STP 410 (American Society for Testing and Materials, Philadelphia PA 1966).
16. ASTM Standard E813-87 in "*Annual Book of ASTM Standards*", Part 10. (American Society for Testing and Materials, Philadelphia PA 1987) p 810.
17. J. R. RICE, *J. Appl. Mech.* **35** (1968) 379.
18. J. A. BEGLEY and J. D. LANDES, *ASTM STP* 514, (American Society for Testing and Materials, Philadelphia PA 1972) p 1
19. J. D. SUMPTER and C. E. TURNER, *Int. J. Fract.* **9** (1973) 320.

Received 25 March
and accepted 21 May 1996